Available online at www.sciencedirect.com
ScienceDirect
Materials Science and Engineering C 28 (2008) 515–518
MATERIALS SCIENCE & ENGINEERING C
www.elsevier.com/locate/msec

Self-supported silver nanoparticles containing bacterial cellulose membranes

Hernane S. Barud [a], Celina Barrios [a], Thais Regiani [a], Rodrigo F.C. Marques [a], Marc Verelst [b], Jeannette Dexpert-Ghys [b], Younes Messaddeq [a], Sidney J.L. Ribeiro [a,*]

[a] *Institute of Chemistry-UNESP, CP 355, Zip 14801-970, Araraquara, SP, 14801-970, Brazil*
[b] *Centre d'Elaboration de Matériaux et d'Etudes Structurales, CEMES, UPR No. 8011 - Université Toulouse III, B.P. 94347, 29 rue Jeanne Marvig, 31055 Toulouse Cedex, France*

Received 26 December 2006; accepted 7 May 2007
Available online 13 May 2007

Abstract

Hydrated bacterial cellulose (BC) membranes obtained from cultures of Acetobacter xylinum were used in the preparation of silver nanoparticles containing cellulose membranes. In situ preparation of Ag nanoparticles was achieved from the hydrolytic decomposition of silver triethanolamine (TEA) complexes. Scanning electron microscopy (SEM) images and X-ray diffraction (XRD) patterns both lead to the observation of spherical metallic silver particles with mean diameter of 8 nm well adsorbed onto the BC fibriles.

Keywords: Bacterial cellulose; Silver; Cellulose membranes; Silver membranes; X-ray diffraction; Electron microscopy

1. Introduction

Cellulose produced by Gram-negative, acetic acid bacteria Acetobacter xylinum (or Gluconaacetobacter xylinus) displays several unique properties when compared to plant cellulose. It is produced as highly hydrated membranes free of lignin and hemicelluloses and displaying higher molecular weight and higher crystallinity, in an ultrafine reticulated structure. A multitude of applications is proposed in industry (paper, textile and food) and as biomaterials in cosmetics and medicine as a consequence of the special properties [1–3]. In fact one of the most promising areas of bacterial cellulose (BC) application as biomaterials is the utilization as a temporary skin substitute in the therapy of difficult wounds, burns and ulcers [1,4–6].

In parallel, thanks to the chemical and structural properties, BC may also be considered as ideal hydrophilic matrix for metals incorporation. Among the different metals possible to be incorporated in BC membranes, silver has attracted renewed interested due to the well known antibacterial properties. This antibacterial activity is being explored commercially in applications such as antibacterial textiles, to prevent infections and to treat burn injuries [7]. The preparation of antimicrobial cellulose acetate nanofibers is described in [8]. In [9] the porous cellulose fibers of plant origin are used as nanoreactors for in situ synthesis of metal nanoparticles. UV radiation or sodium boron hydride ($NaBH_4$) are used as reducing agents. The interaction mechanism between silver ions and functional groups in microcrystalline cellulose, in the presence of different reducing agents, is discussed in [10]. Concerning BC, Baklagina et al have described the effects of the incorporation of polyvinylpyrrolidone and poviargol on the preparation of BC- silver membranes [11]. The aim of the present work lies on the preparation of self-supported bacterial cellulose membrane containing silver nanoparticles. In situ silver ions reduction by the chelating-reducing agent triethanolamine (TEA) is described.

2. Experimental

Analytical grade reactants were used as received. Bacterial cellulose membranes obtained from Acetobacter xylinum cultures (1 cm^2) were soaked for 10 min in 10 ml of 0.01 mol L^{-1} $AgNO_3$ solution. 0.1 ml of 0.01 mol L^{-1} TEA solution were added and the mixture left for 12 h. After that, samples

* Corresponding author.
E-mail address: sidney@iq.unesp.br (S.J.L. Ribeiro).

0928-4931/$ - see front matter © 2007 Elsevier B.V. All rights reserved.
doi:10.1016/j.msec.2007.05.001

were washed several times in water and refluxed in 10 ml of ethanol solution 30% (weight/volume) at 80 °C. Resulting membranes were dried in air at 100 °C.

Scanning electron microscopy (SEM) images were obtained in a Field Emission Scanning Electron Microscopy JEOL JMF-6700F model. Samples were coated with a 1 nm thick gold layer.

X-ray diffraction patterns (XRD) were obtained in a Siemens Kristalloflex diffractometer using nickel filtered Cu K_α radiation from 4 to 70° (2θ angle).

Thermal gravimetric (TG) curves were obtained for dried samples in a SDT 2960 equipment from TA-Instruments. Samples were heated in open alumina pans from 40 to 500 °C, under nitrogen atmosphere, 70 mL min^{-1}, at heating rate of 10 °C min^{-1}.

3. Results and discussion

Macroscopically transparent and homogenous membranes were obtained, yellow to grey colored depending on the silver content that could be controlled from the silver solution concentration. In the following results obtained with 10 ml of the 0.01 mol L^{-1} $AgNO_3$ solution will be shown. Fig. 1 shows SEM images of the pure bacterial cellulose membranes (Fig. 1a) and those obtained from the Ag–TEA treatment (Fig. 1b,c and d). Fig. 1a shows aggregates of semi crystalline extended cellulose chains in an ultrafine network structure. This sponge-like structure consists of continuous nanofibers about 10 nm ticks and 50 nm wide.

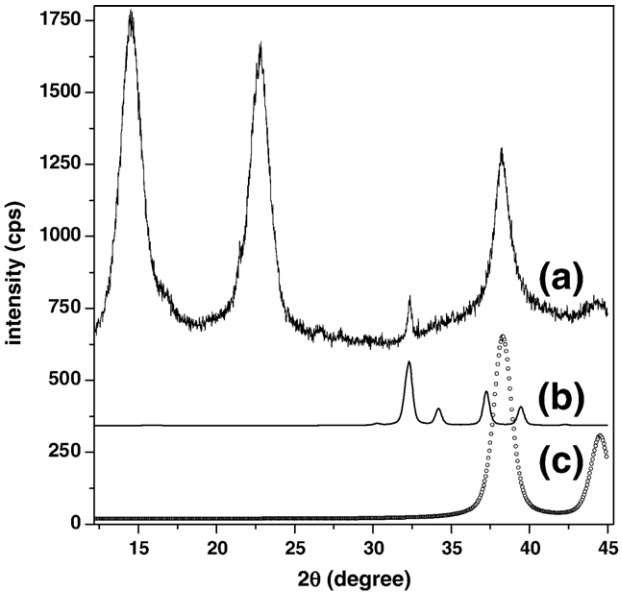

Fig. 2. X-rays diffraction patterns. a) Experimental diffraction pattern obtained for BC–Ag–TEA membrane; generated patterns for AgO (b) and Ag (c) as described in the text.

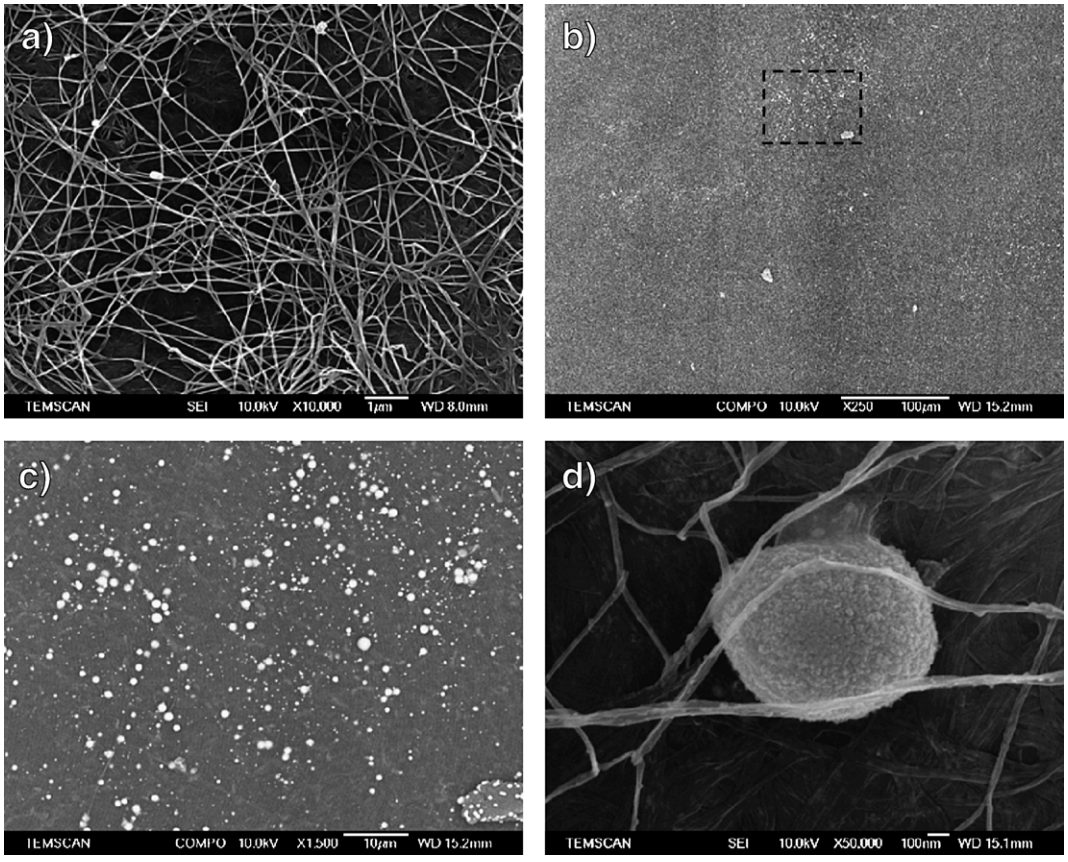

Fig. 1. SEM images. a) Pure BC membrane. Bar — 1 μm; b) silver containing membrane (secondary electrons image). Bar — 100 m; c) magnified area marked as a rectangle in b) where silver particles are identified as white spots. Bar — 10 μm; d) single silver nanoparticle agglomerate wrapped by BC fibriles. Bar — 100 nm.

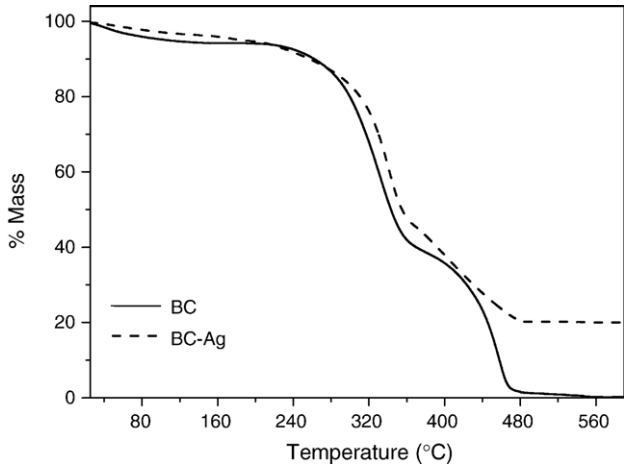

Fig. 3. TG curves obtained for pure BC and BC–Ag membranes.

A general view of the BC–Ag–TEA membranes surface is presented in Fig. 1b, which is an image obtained with secondary electrons. In this detection mode silver particles are highlighted due to higher atomic weight. The marked rectangle is magnified in Fig. 1c. BC–Ag–TEA membranes present regular surface morphology and Fig. 1c shows clearly well dispersed spherical silver particles (white spots) in the BC membrane. Nanometric particles in fact show up also as bigger aglomerates and Fig. 1d shows one spherical Ag agglomerate grain wrapped by the BC fibers. Smaller silver particles that compose the grain are also observed adsorbed on the fibriles surface. A strong silver–BC interaction is in fact deduced from these images and also from the preparation routine where samples were water–ethanol washed several times in order to remove free silver ions.

Fig. 2 shows XRD patterns of one typical BC–Ag–TEA membrane together with the XRD patterns of Ag and Ag oxide phases obtained from ICSD [12] and generated using the GSAS software, with bandwidths artificially fitting the experimental ones [13]. Broad diffraction peaks at 15 and 22.5° are assigned to the characteristic interplane distances of cellulose 1_α and 1_β phases ($100_{1\alpha}$, $110_{1\beta}$ and $010_{1\beta}$ planes at 15° and $110_{1\alpha}$ and $200_{1\beta}$ at 22.5°). Ag cubic phase was clearly identified from diffraction peaks at 38.3° and 44.5° (crystallographic planes (111) and (220), respectively). The mean particle size of Ag nanoparticles was calculated from the full width at half maximum (FWHM) of (111) peak using Scherer formula and was equal to 8.5 nm. It should be noted that silver diffraction peaks could only be clearly observed when TEA was used in the preparation procedure.

A peak at 32.3° that does not correspond to any BC or Ag diffraction peaks is also observed. As Fig. 2 shows it could be ascribed either to AgO or Ag_2O phases [14].

Fig. 3 shows TG curves obtained for BC and BC–Ag membranes. The thermal degradation of BC occurs in two steps located at approximately 330 °C and 460 °C. The residual mass (21%) obtained for temperatures above 600 °C is related to silver particles.

The formation of Ag nanoparticles on BC fibers can be explained in terms of the interaction with cellulose hydroxyl groups. Despite of the fact that cellulose structure exhibits aldehyde hydrates reducing terminal groups, no metallic silver peak could be observed in XRD patterns of membranes prepared only from BC and Ag^+ solutions. Diffusion of hydrated silver ions $[Ag(H_2O)_2]^+$ into bacterial cellulose matrix leads to coordination with the different cellulose hydroxyl groups. In general the reducing action of different agents (UV radiation, sodium boron hydride, hypophosphite among others) is required [8–11]. In this work the additional interaction with TEA should lead to a more complex reduction mechanism. TEA molecules act simultaneously as a strong reducing agent and good silver ions chelating agent, influencing the nucleation and particle growth, hence particle size. Hydrolytic decomposition of Ag–TEA complexes in aqueous solutions at around 50 °C is known to lead to Ag and AgO thin films [14]. TEA acts as a tridentate ligand through two of the three hydroxyl O atoms together with the amine N atom. Ag^+ is reduced to $Ag(0)_2$ and once these particles are formed, they act as a catalyst for the reduction of the remaining metal ions present in the bulk solution leading to $Ag(0)_n$ cluster growth. The aggregation process does not cease until all metal ions in solutions are consumed, resulting in larger particles [14]. In this work the homogenous distribution of silver nanoparticles with mean size of 8.5 nm suggests that cellulose fibers act as a template for Ag(0) deposition. The hydrolytic decomposition of the Ag–TEA complexes lead to silver particles formation stabilized on the BC fibriles. Moreover, in Ag^+ excess, Ag^+ ions could be sandwiched by two TEA molecules, as illustrated in Fig. 4(a). Intra and intermolecular hydrogen bonding among hydroxyl TEA groups could lead to a three-dimensional network (Fig. 4(b))

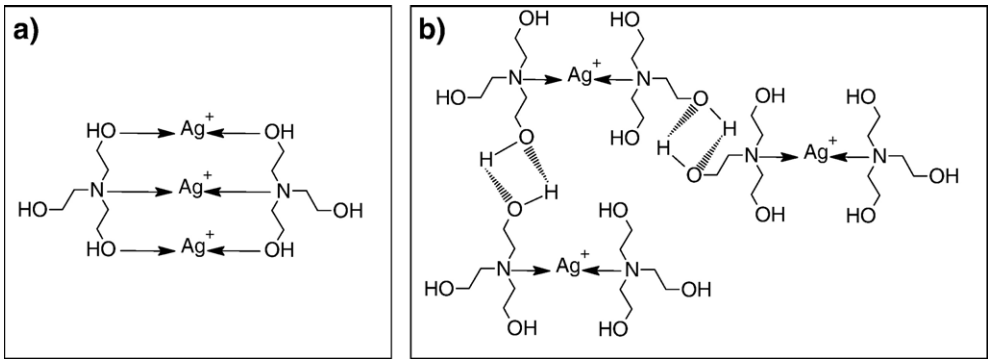

Fig. 4. Schematic representation of the TEA–Ag interaction. a) in excess Ag^+; b) Hydrogen bonding of different Ag–TEA complexes.

and the decomposition of this three-dimensional complex network allows the sphere precipitation on BC surface.

The observation of AgO phase in XRD diffraction pattern corroborates the decomposition mechanism for Ag–TEA complexes proposed in [14] since the low TEA/Silver concentration used here (1:100) should lead to a Ag(0)–AgO mixture. The hydrogen bonding interaction between 3D Ag^{+}–TEA structure and BC fiber must be taken into account to explain the spherical-particle/BC-fiber interaction verified in Fig. 1d. The systematic evaluation of different Ag–TEA concentration and antibacterals tests are under study in our laboratory.

4. Conclusion

Transparent, macroscopically homogeneous silver containing bacterial cellulose (BC) membranes were obtained from BC hydrated membranes obtained from Acetobacter xylinum cultures, soaked on Ag^{+}-TEA solutions. Electron microscopy images and XRD diffraction patterns both lead to the observation of metallic silver particles with mean diameter of 8 nm well adsorbed onto the BC fibriles. The utilization of TEA as stabilizer and reducing agent leads to spherical particles well dispersed on the BC bulk ultrafine reticulated structure. The potential use of such membranes in antibacterial applications could be foreseen and will the subject of future publications.

Acknowledgments

Authors acknowledge the financial support of Brazilian agencies FAPESP and CNPq. The financial support of the bilateral research cooperation program between the Brazilian CAPES and French COFECUB agencies is also acknowledged.

References

[1] S. Bielecki, A. Krystynowicz, M. Turkiewicz, H. Kalinowska, Bacterial Cellulose (Ch. 14) p.381 in: Biotechnology of biopolymers. From synthesis to patents, Ed. Steinbuchel, A. and Doi, Y., Wiley-VCH Verlag GmbH, Weinheim, 2005.
[2] D. Klemm, B. Heublein, H.-P. Fink, A. Bohn, A. Angew. Chem., Int. Ed. 44 (2005) 3358.
[3] M. Iguchi, S. Yamanaka, A. Budhiono, J. Mater. Sci. 35 (2000) 261.
[4] R.L. Sheridan, J.R. Morgan, R. Mohamed, Biomaterials in burn and wound dressings, Ch. 17, in: D. Severian (Ed.), Handbook of Polymeric Biomaterials, Marcel Dekker, New York, 2002, p. 451.
[5] J.D. Fontana, A.M. de Souza, C.K. Fontana, I.L. Torriani, J.C. Moreschi, B.J. Gallotti, S.J. de Souza, G.P. Narcisco, J.A. Bichara, L.F. Farah, Appl. Biochem. Biotechnol. 24/25 (1990) 253.
[6] R. Jonas, L.F. Farah, Polym. Degrad. Stab. 59 (1998) 101.
[7] P.L. Taylor, A.L. Hussher, R.E. Burrel, Biomaterials 26 (2005) 7221.
[8] W.K. Son, J.H. Youk, W.H. Park, Carbohydr. Polym. 65 (2006) 430.
[9] J. He, T. Kunitake, A. Naiko, Chem. Mater. 15 (2003) 4401.
[10] N.E. Kotelnikova, V.N. Demidov, G. Wegener, E. Windeisen, Russ. J. Gen. Chem. 73 (3) (2003) 427.
[11] Y.G. Baklagina, A.K. Khripunov, A.A. Tkachenko, V.V. Kopeikin, N.A. Matveeva, V.K. Lavrent'ev, V.K. Nilova, T.E. Sukhanova, R.Y. Smyslov, I.S. Zanaveskina, V.V. Klechkovskaya, L.A. Feigin, Russ. J. Appl. Chem. 78 (7) (2005) 1176.
[12] Inorganic Crystal Structure Database, ICSD, 2002.
[13] A.C. Larson, R.B. Von Dreele, Los Alamos National Laboratory. Los Alamos, EUA. Copyright, 1985–2000, The Regents of the University of California, 2001.
[14] T. Kocareva, I. Grozdanov, B. Pejova, Mater. Lett. 47 (2001) 319.